Journal of Computational and Applied Mathematics 42 (1992) 49–61
North-Holland

CAM 1181

On the numerical solution of the three-dimensional inverse obstacle scattering problem

Rainer Kress and Axel Zinn
Institut für Numerische und Angewandte Mathematik, Universität Göttingen, Germany

Received 21 February 1991
Revised 3 June 1991

Abstract

Kress, R. and A. Zinn, On the numerical solution of the three-dimensional inverse obstacle scattering problem, Journal of Computational and Applied Mathematics 42 (1992) 49–61.

The inverse problem under consideration is to determine the shape of an impenetrable sound-soft obstacle from the knowledge of a time-harmonic incident plane acoustic wave and far-field or near-field measurements of the scattered wave. We present a method for the approximate solution which avoids the solution of the corresponding direct problem and stabilizes the ill-posed inverse problem by reformulating it as a nonlinear optimization problem. The numerical implementation of the method is described and some three-dimensional examples of reconstructions are given.

Keywords: Time-harmonic acoustic obstacle scattering, Helmholtz equation, inverse problem, optimization method, numerical approximation.

1. The inverse scattering problem

The scattering of time-harmonic acoustic waves by an impenetrable sound-soft obstacle D, that is, a bounded domain $D \subset \mathbb{R}^3$ imbedded in a homogeneous isotropic medium, leads to an exterior boundary value problem for the Helmholtz equation

$$\Delta u + k^2 u = 0, \quad \text{in } \mathbb{R}^3 \setminus \overline{D}, \tag{1.1}$$

with positive wave number k and Dirichlet boundary condition

$$u = 0, \quad \text{on } \partial D. \tag{1.2}$$

The total wave $u = u^i + u^s$ is decomposed into the given incident plane wave $u^i(x) = e^{ikd \cdot x}$,

Correspondence to: Prof. R. Kress, Institut für Numerische und Angewandte Mathematik, Universität Göttingen, Lotzestrasse 16–18, W-3400 Göttingen, Germany.

where d is a unit vector giving the direction of propagation, and the unknown scattered wave u^s which is required to satisfy the Sommerfeld radiation condition

$$\frac{\partial u^s}{\partial r} - iku^s = o\left(\frac{1}{r}\right), \quad r = |x| \to \infty, \tag{1.3}$$

uniformly in all directions $\hat{x} = x/|x|$. This radiation condition ensures the uniqueness for the exterior boundary value problem and leads to an asymptotic behaviour of the form

$$u^s(x) = \frac{e^{ik|x|}}{|x|}\left\{u_\infty(\hat{x}) + O\left(\frac{1}{|x|}\right)\right\}, \quad |x| \to \infty, \tag{1.4}$$

uniformly in all directions $\hat{x} = x/|x|$, where the function u_∞, defined on the unit sphere Ω in $\mathbb{R}^3$, is known as the far-field pattern or scattering amplitude of the scattered wave. A vanishing far-field pattern $u_\infty = 0$ on the unit sphere implies

$$\lim_{r\to\infty} \int_{|x|=r} |u^s(x)|^2 \, ds = 0,$$

whence $u^s = 0$ follows by Reilich's lemma (see [2]). That means, there is a one-to-one correspondence between the scattered wave u^s and its far-field pattern u_∞.

As in classical potential theory, for smooth boundaries, existence of a solution for the exterior Dirichlet problem (1.1)–(1.3) can be based on boundary integral equations. For details we refer to [2]. The continuous dependence of the solution on the boundary ∂D can be shown either by integral equation methods as in [1] or by weak solution techniques as in [15]. Since a proof by the second possibility has not yet appeared in the literature, for convenience, we include an outline and state the following theorem.

Theorem 1.1. *The mapping $\partial D \mapsto u_\infty$ is continuous from C^1 into $L^2(\Omega)$.*

Proof. Choose R large enough such that D is contained in the sphere Ω_R of radius R centered at the origin and denote $D_R := \{x \in \mathbb{R}^3 \setminus \overline{D}: |x| < R\}$. Introduce the Sobolev space $\tilde{H}_0^1(D_R) := \{v \in H^1(D_R): v = 0 \text{ on } \partial D\}$. Then, by Green's theorem, we derive that the solution u to the direct scattering problem satisfies

$$\int_{D_R} \{\text{grad } u \cdot \text{grad } \bar{v} - k^2 u\bar{v}\} \, dx = \int_{\Omega_R} \frac{\partial u}{\partial \nu}\bar{v} \, ds, \tag{1.5}$$

for all $v \in \tilde{H}_0^1(D_R)$ where ν denotes the exterior unit normal.

By $L: H^{-1/2}(\Omega_R) \to H^{1/2}(\Omega_R)$ we denote the Neumann to Dirichlet map for solutions w to the Helmholtz equation in the exterior of Ω_R which satisfy the Sommerfeld radiation condition. It transforms the normal derivative on the boundary into the boundary values

$$L: \frac{\partial w}{\partial \nu} \mapsto w, \quad \text{on } \Omega_R.$$

The properties of the operator L can be investigated by boundary integral equation methods or, for the simple shape of the sphere, by expansion of w with respect to spherical wave functions. From the expansion

$$w(x) = \sum_{n=0}^{\infty} \sum_{m=-n}^{n} a_n^m h_n^{(1)}(k|x|) Y_n^m(\hat{x}), \quad |x| > R,$$

where $h_n^{(1)}$ denotes the spherical Hankel function of order n and of the first kind and where Y_n^m, $m = -n, \ldots, n$, denotes an orthonormal set of spherical harmonics of order n, it readily follows that L maps

$$g = \sum_{n=0}^{\infty} \sum_{m=-n}^{n} b_n^m Y_n^m \quad \text{into} \quad Lg = \sum_{n=0}^{\infty} \sum_{m=-n}^{n} \gamma_n b_n^m Y_n^m,$$

where the coefficients γ_n are given by

$$\gamma_n := \frac{h_n^{(1)}(kR)}{kh_n^{(1)'}(kR)}, \quad n = 0, 1, \ldots .$$

Since $\gamma_n \neq 0$ for all n, the operator L clearly is bijective. From the power series expansion for the spherical Hankel functions, for fixed k, we derive

$$\gamma_n = -\frac{R}{n+1}\left\{1 + O\left(\frac{1}{n}\right)\right\}, \quad n \to \infty.$$

This implies that L is bounded and has a bounded inverse from $H^{1/2}(\Omega_R)$ onto $H^{-1/2}(\Omega_R)$. After denoting the operator L in the limiting case $k = 0$ by L_0, in addition, from

$$\lim_{k \to 0} \gamma_n = -\frac{R}{n+1},$$

which is valid uniformly for all n, and the above asymptotics for γ_n, we can conclude that the difference $L - L_0$ is compact from $H^{-1/2}(\Omega_R)$ into $H^{1/2}(\Omega_R)$. Finally, since

$$-\int_{\Omega_R} L_0 g \bar{g} \, ds = R \sum_{n=0}^{\infty} \sum_{m=-n}^{n} \frac{1}{n+1} |b_n^m|^2,$$

that is,

$$-\int_{\Omega_R} L_0 g \bar{g} \, ds \geqslant c \| g \|_{H^{-1/2}(\Omega_R)},$$

with some constant $c > 0$, we observe that the operator $-L_0$ is strictly coercive.

From (1.5) now it can be deduced that for the solution to the scattering problem, $u \in \tilde{H}_0^1(D_R)$ and $g = \partial u^s / \partial \nu \in H^{-1/2}(\Omega_R)$ satisfy the sesquilinear equation

$$\int_{D_R} \{\operatorname{grad} u \cdot \operatorname{grad} \bar{v} - k^2 u \bar{v}\} \, dx - \int_{\Omega_R} g \bar{v} \, ds - \int_{\Omega_R} (Lg - u) \bar{h} \, ds$$

$$= \int_{\Omega_R} \left\{ \frac{\partial u^i}{\partial \nu} \bar{v} + u^i \bar{h} \right\} ds, \tag{1.6}$$

for all $v \in \tilde{H}_0^1(D_R)$ and $h \in H^{-1/2}(\Omega_R)$. The sesquilinear form S defined on $\tilde{H}_0^1(D_R) \times H^{-1/2}(\Omega_R)$ by the left-hand side of (1.6) can be decomposed into $S = S_0 + S_1$, where

$$S_0(u, g; v, h) := \int_{D_R} \operatorname{grad} u \cdot \operatorname{grad} \bar{v} \, dx - \int_{\Omega_R} \{g \bar{v} - u \bar{h}\} \, ds - \int_{\Omega_R} L_0 g \bar{h} \, ds$$

is strictly coercive, and where

$$S_1(u, g; v, h) := -k^2 \int_{D_R} u \bar{v} \, dx - \int_{\Omega_R} (L - L_0) g \bar{h} \, ds$$

is compact. Hence, by the Lax–Milgram theorem and the Riesz theory for compact operators, the unique solvability of the direct scattering problem implies unique solvability of the sesquilinear equation (1.6) and continuous dependence of the solution on the right-hand side. In particular, the solution operator

$$A: u^i \mapsto g = \frac{\partial u^s}{\partial \nu} \tag{1.7}$$

is continuous from $H^{1/2}(\Omega_R)$ into $H^{-1/2}(\Omega_R)$.

Now we wish to study the dependence of the sesquilinear form S on the shape of the domain D. For this we restrict ourselves to the case of domains which are starlike with respect to the origin. Assume that ∂D is represented in the parametric form

$$x(\theta) = r(\theta)\theta, \quad \theta \in \Omega,$$

with a positive function $r \in C^2(\Omega)$. We pick $R = 2 \cdot \max\{1, \|r\|_\infty\}$. Then the mapping

$$f(t, \theta) := \begin{cases} \left[t + (r(\theta) - 1)\left(\frac{R - t}{R - 1} \right)^2 \right] \theta, & 1 \leqslant t \leqslant R, \quad \theta \in \Omega, \\ t\theta, & R \leqslant t < \infty, \quad \theta \in \Omega, \end{cases}$$

is a diffeomorphism from the exterior of the unit sphere onto $\mathbb{R}^3 \setminus D$ such that $\{y \in \mathbb{R}^3: 1 < |y| < R\}$ is mapped onto D_R. Denote by

$$y(x) = (y_1(x), y_2(x), y_3(x))$$

the inverse map expressed in Cartesian coordinates. Then we substitute to obtain

$$\int_{D_R} \{\operatorname{grad} u \cdot \operatorname{grad} \bar{v} - k^2 u \bar{v}\} \, dx = \int_{1 \leqslant |y| \leqslant R} \left\{ \sum_{j,k=1}^{3} a_{jk} \frac{\partial u}{\partial y_j} \frac{\partial \bar{v}}{\partial y_k} - k^2 u \bar{v} \right\} J \, dy, \tag{1.8}$$

where J denotes the Jacobian of the substitution and where the coefficients a_{jk} are given by

$$a_{jk} = \sum_{i=1}^{3} \frac{\partial y_j}{\partial x_i} \frac{\partial y_k}{\partial x_i}.$$

As is easily seen, J and a_{jk} depend continuously on r in the C^1-norm. Hence, from (1.8) we deduce that after the transformation the sesquilinear S also depends continuously on r with respect to the C^1-norm. Therefore, a perturbation argument based on the Neumann series shows that the operator A introduced through (1.7) satisfies an inequality of the form

$$\|A_r - A_{r+q}\| \leqslant C_1(r) \|q\|_{C^1(\Omega)},$$

for all sufficiently small $q \in C^2(\Omega)$ with some constant C_1 depending on r. Hence it follows that

$$\left\| \frac{\partial u_r^s}{\partial \nu} - \frac{\partial u_{r+q}^s}{\partial \nu} \right\|_{H^{-1/2}(\Omega_R)} \leqslant C_2(r) \|q\|_{C^1(\Omega)},$$

and consequently

$$\|u_{\infty,r} - u_{\infty,r+q}\|_{L^2(\Omega)} \leqslant C_3(r) \|q\|_{C^1(\Omega)},$$

with constants C_2 and C_3. Now the proof is finished. □

The *inverse problem* we are concerned with is, given the far-field pattern u_∞ of the scattered wave u^s for one incoming plane wave u^i with one single incident direction d and one single wave number k or possibly several incoming plane waves u^i with different incident directions d and wave numbers k, to determine the shape of the scatterer D. In addition to the reconstruction of D from far-field data we also want to consider the reconstruction from measurements of the scattered wave u^s on some closed surface Γ_{meas} containing D in its interior.

As opposed to the direct problem, both these inverse problems are ill-posed. The solution — if it exists at all — does not depend continuously on the given far-field or near-field data in any reasonable norm. Therefore the numerical solution requires the incorporation of some regularization technique. In addition, the inverse scattering problem is nonlinear since the scattered wave depends nonlinearly on the boundary surface.

Based on a result due to Schiffer, the question of uniqueness has been revisited in [6,7]. Given a priori information on the size of the obstacle, the far-field pattern of a finite number of incident plane waves *either* with one fixed incident direction and different wave numbers *or* with one fixed wave number and different incident directions uniquely determines D. Note that due to analyticity, theoretically, it suffices to know the far-field pattern for a countable set of observation directions $\hat{x}$. It is still an open problem whether one incoming plane wave for one single direction and one single wave number completely determines the scatterer.

By the uniqueness for the exterior Dirichlet problem, knowing u^s on the closed surface Γ_{meas} implies knowing the far-field pattern u_∞ of u^s. Therefore the uniqueness results for the reconstruction from far-field data immediately carry over to the case of near-field data.

In this paper we are interested in the approximate solution of the inverse problem for wave numbers k in the resonance region, that is, the wave length is of the same magnitude as the diameter of the unknown object. In this case linearizations by high-frequency asymptotics like geometric and physical optics do not lead to valid approximations and it is necessary to treat the full nonlinear problem.

2. A numerical algorithm for the inverse problem

An obvious concept for an approximate solution of the inverse scattering problem is to try solving the ill-posed nonlinear operator equation

$$A(\partial D) = u_\infty, \tag{2.1}$$

by standard inversion methods. Here $A: X \to L^2(\Omega)$ stands for the forward operator mapping the boundary ∂D into the far-field pattern u_∞ of the scattered wave and X is a suitably chosen subset of a suitable function space representing the boundary surfaces.

Newton-type methods for the approximate solution of (2.1) have been implemented in [13,14,16,17]. The ill-posedness of the inverse scattering problem requires appropriate measures to stabilize the Newton iteration, for example by a Tikhonov regularization or a singular-value cut-off in each Newton step.

The method of quasi solutions has been investigated in [1]. Here the inverse scattering problem is replaced by minimizing the defect

$$\| A(\Lambda) - u_\infty \|_{L^2(\Omega)}, \tag{2.2}$$

over all admissible surfaces Λ in a suitable compact set U. A Tikhonov-type regularization of the defect minimization (2.2) has been employed in [11]. Here the constraint for the admissible subset U to be compact is replaced by minimizing a penalized defect functional of the form

$$\| A(\Lambda) - u_\infty \|_{L^2(\Omega)} + p(\Lambda), \tag{2.3}$$

with a suitable penalty term p.

A common feature of all the above methods is that they are of an iterative nature and require the numerical solution of the direct scattering problem for different domains at each iteration step. In addition, to date, numerical experiments with these methods have only been performed in two dimensions. The method which we describe in the sequel and which was proposed by Kirsch and Kress [8] does not need the solution of the direct problem at all. The principal idea is to stabilize the inverse scattering problem by reformulating it as a nonlinear optimization problem. Our method is closely related to an approach proposed by Colton and Monk in a series of papers [3–5]. The Colton–Monk method so far is the only one by which numerical reconstructions in the resonance region have been carried out in three dimensions [5]. For a comparison of both methods including numerical examples in two dimensions we refer to [9]. The three-dimensional Colton–Monk method has also been implemented and tested in [12].

Of course, the numerical solution of the optimization problem again relies on iteration techniques. However, the actual performance of these iterations is less costly due to the simple structure of the cost functional. The motivation of the Kirsch–Kress method is divided into two parts: the first part deals with the ill-posedness and the second part with the nonlinearity of the inverse scattering problem.

We choose an auxiliary closed surface Γ contained in the unknown scatterer D. The knowledge of such an internal surface Γ requires weak a priori information about D. Without loss of generality we may assume that Γ is chosen such that the Helmholtz equation $\Delta u + k^2 u = 0$ in the interior of Γ with homogeneous boundary condition $u = 0$ on Γ admits only the trivial solution $u = 0$. For example, we may choose Γ to be a sphere of radius R such that kR is not a zero of a spherical Bessel function. We try to represent the scattered field $u^s = S\phi$ as an acoustic single-layer potential

$$(S\phi)(x) := \int_\Gamma \frac{e^{ik|x-y|}}{|x-y|} \phi(y)\, ds(y), \tag{2.4}$$

with an unknown density $\phi \in L^2(\Gamma)$. Since the far-field pattern of the single-layer potential is described through the integral operator $F: L^2(\Gamma) \to L^2(\Omega)$ defined by

$$(F\phi)(\hat{x}) := \int_\Gamma \phi(y)\, e^{-ik\hat{x}\cdot y}\, ds(y), \quad \hat{x} \in \Omega, \tag{2.5}$$

given the far-field pattern u_∞, we have to solve the integral equation of the first kind

$$F\phi = u_\infty, \tag{2.6}$$

for the density ϕ. The integral operator F has a smooth kernel and therefore (2.6) is severely ill-posed. It can be shown that (2.6) has at most one solution and that it is solvable if and only if u_∞ is the far-field of a scattered wave which can be analytically extended as a solution to the Helmholtz equation across the boundary ∂D into the exterior of Γ with boundary data in the Sobolev space $H^1(\Gamma)$ (see [10] for the two-dimensional case).

We may apply the Tikhonov regularization technique (see [10]) for a stable numerical solution of (2.6) and obtain an approximation $u^s_{approx} = S\phi_{approx}$ for the scattered field by the single-layer potential (2.4). Then we seek the boundary of the scatterer D as the location of the zeros of $u^i + u^s_{approx}$ in a minimum norm sense, i.e., we approximate ∂D by minimizing the defect

$$\|u^i + u^s_{approx}\|_{L^2(\Lambda)} \tag{2.7}$$

over some suitable class U of admissible surfaces Λ. For example, we may choose U to be a suitable subset of the set V of all starlike closed C^2-surfaces Λ described by

$$x(\theta) := r(\theta)\theta, \quad \theta \in \Omega, \ r \in C^1(\Omega), \tag{2.8}$$

which is compact in $C^{1,\beta}$ with some $0 < \beta < 1$. In addition, we assume the surfaces in U to satisfy some a priori information

$$0 < r_1(\theta) \leq r(\theta) \leq r_2(\theta), \quad \theta \in \Omega, \tag{2.9}$$

with given functions r_1 and r_2.

However, in general we do not have the existence of a solution to the integral equation (2.6). Therefore, for a satisfactory reformulation of the inverse scattering problem by an optimization problem we combine the Tikhonov regularization for (2.6) and the defect minimization (2.7) into one cost functional. Given u^i and u_∞, we minimize the sum

$$\mu(\phi, \Lambda; \alpha, \gamma) := \|F\phi - u_\infty\|^2_{L^2(\Omega)} + \alpha\|\phi\|^2_{L^2(\Gamma)} + \gamma\|u^i + S\phi\|^2_{L^2(\Lambda)}, \tag{2.10}$$

simultaneously over all $\phi \in L^2(\Gamma)$ and $\Lambda \in U$. Here, $\alpha > 0$ denotes the regularization parameter for the Tikhonov regularization of (2.6) represented by the first two terms in (2.10) and $\gamma > 0$ denotes a coupling parameter which has to be chosen appropriately for the numerical implementation. The following existence and convergence results were established in [8]. For a proof — it partly relies on continuous dependence results similar to those of Theorem 1.1 — we also refer to [10].

Theorem 2.1. *The optimization formulation of the inverse scattering problem has a solution.*

If u_∞ is the exact far-field pattern of a domain D with $\partial D \in U$, then for the cost functional there holds convergence:

$$\inf_{\phi \in L^2(\Gamma), \Lambda \in U} \mu(\phi, \Lambda; \alpha, \gamma) \to 0, \quad \alpha \to 0,$$

and for any sequence (ϕ_n, Λ_n) of solutions with parameters $\alpha_n \to 0$, $n \to \infty$, there exists a convergent subsequence of (Λ_n) and on each limit surface Λ the exact total field $u^i + u^s$ vanishes.

Since we do not have uniquencss either for the inverse scattering problem or for the optimization problem, in general, we cannot expect more than convergent subsequences. In addition, due to the lack of a uniqueness result for one wave number and one incident plane wave, we cannot assure that we always have convergence towards the boundary of the unknown scatterer. The latter insufficiency can be removed by using more incident waves $u^i_1, \ldots, u^i_n$ with different directions $d_1, \ldots, d_n$ with corresponding far-field patterns $u_{\infty,1}, \ldots, u_{\infty,n}$ with the total

number n depending on the size of the a priori known surfaces Λ_1 and Λ_2. Then we have to minimize the sum

$$\sum_{j=1}^{n} \left\{ \| F\phi_j - u_{\infty,j} \|^2_{L^2(\Omega)} + \alpha \| \phi_j \|^2_{L^2(\Gamma)} + \gamma \| u^i_j + S\phi_j \|^2_{L^2(\Lambda)} \right\}, \tag{2.11}$$

over all $\phi_1, \ldots, \phi_n \in L^2(\Gamma)$ and all $\Gamma \in U$. Of course, we also can expect more accurate reconstructions by using more than one incoming direction at the price of an increase in the computational costs. These costs can be reduced by using appropriate linear combinations of incident plane waves as suggested in [19].

In the case of near-field measurements u^s_{meas} on the surface Γ_{meas} the integral equation (2.6) has to be replaced by

$$\tilde{F}\phi = u^s_{\text{meas}}, \tag{2.12}$$

where the integral operator $\tilde{F}: L^2(\Gamma) \to L^2(\Gamma_{\text{meas}})$ is given by

$$(\tilde{F}\phi)(x) := \int_\Gamma \frac{e^{ik|x-y|}}{|x-y|} \phi(y)\, ds(y), \quad x \in \Gamma_{\text{meas}}. \tag{2.13}$$

Correspondingly, for given u^i and u^s_{meas}, the optimization problem (2.10) has to be modified into minimizing the sum

$$\| \tilde{F}\phi - u^s_{\text{meas}} \|^2_{L^2(\Gamma_{\text{meas}})} + \alpha \| \phi \|^2_{L^2(\Gamma)} + \gamma \| u^i + S\phi \|^2_{L^2(\Lambda)}, \tag{2.14}$$

simultaneously over all $\phi \in L^2(\Gamma)$ and $\Lambda \in U$. Then the results of Theorem 2.1 carry over to the near-field case.

So far we have assumed the far-field to be known for all observation directions $\hat{x}$. Theoretical and numerical extensions to the case where the far-field pattern is measured only on part of the unit sphere, that is, to the limited-aperture problem, were considered in [19].

3. Numerical implementation and results

We proceed describing some details of the numerical implementation of the above method. For the data we have to rely on synthetic far-field data obtained through the numerical solution of the direct scattering problem. Here we wish to emphasize that for reliably testing the performance of the approximation method for the inverse problem, it is crucial that the synthetic data are delivered through a direct solver which has no connection to the inverse solver under consideration, in order to avoid trivial inversion of finite-dimensional problems. In our numerical examples the far-field data were obtained through the classical boundary integral equations via the combined double- and single-layer approach (see [2]). For its numerical solution we employed a Nyström-type method using numerical quadratures based on approximations through spherical harmonics. This method is exponentially convergent for smooth boundaries and has been recently developed in [18].

For the numerical method for the inverse problem, the evaluation of the cost functional (2.10) or (2.14) including the integral operators S, F and $\tilde{F}$ requires the numerical evaluation of integrals with integrands over the smooth surfaces Ω, Γ, Γ_{meas} and Λ. We approximate

integrals over the unit sphere by the Gauss trapezoidal product rule. By $-1 < t_1 < t_2 < \cdots < t_m < 1$ we denote the zeros of the Legendre polynomial P_m and by

$$\alpha_j := \frac{2}{\left(1-t_j^2\right)\left[P_m'(t_j)\right]^2}, \quad j = 1, \ldots, m,$$

the weights of the Gauss–Legendre quadrature rule for the interval $[-1,1]$. Then the Gauss trapezoidal rule reads

$$\int_\Omega f \, ds \approx \frac{\pi}{m} \sum_{j=1}^{m} \sum_{k=0}^{2m-1} \alpha_j f(x_{jk}), \tag{3.1}$$

where the knots x_{jk} are given in spherical coordinates by

$$x_{jk} := (\sin \theta_j \cos \phi_k, \sin \theta_j \sin \phi_k, \cos \theta_j)$$

for $j = 1, \ldots, m$ and $k = 0, \ldots, 2m-1$ with $\theta_j := \arccos t_j$ and $\phi_k = \pi k/m$. Integrals over the surfaces Γ, Γ_{meas} and Λ are transformed into integrals over Ω through appropriate substitutions.

For the numerical solution, of course, we also must discretize the optimization problem. This is achieved through replacing $L^2(\Gamma)$ and U by finite-dimensional subspaces. Denote by Z_n the linear space of all spherical harmonics of order less than or equal to n. Let $q: \Gamma \to \Omega$ be bijective and define $X_n \subset L^2(\Gamma)$ by

$$X_n := \{\phi = Y \circ q : Y \in Z_n\}.$$

Further we denote by U_n the set of all starlike surfaces described through (2.8) and (2.9) with $r \in Z_n$. Then we replace (2.10) or (2.14), respectively, by the finite-dimensional problem where we minimize over the finite-dimensional set $X_n \times U_n$ instead of $L^2(\Gamma) \times U$. Denoting by μ_n and μ the infimum of the corresponding optimization problems, we can establish the following convergence result.

Theorem 3.1. *Denote by* (ϕ_n, Λ_n) *for* $n \in \mathbb{N}$ *a solution to the finite-dimensional minimization problem. Then there holds* $\mu_n \to \mu$, $n \to \infty$, *and there exists a subsequence* $(\phi_{n(j)}, \Lambda_{n(j)})$ *which converges to a solution of* (2.10) *or* (2.14), *respectively, as* $j \to \infty$.

Proof. (We only give a sketch, for a detailed version see [20].) Let (ϕ^*, Λ^*) be a solution to (2.10) or (2.14). Then, omitting the dependence on α and γ, we have

$$\mu(\phi^*, \Lambda^*) = \mu \leqslant \mu_n = \mu(\phi_n, \Lambda_n).$$

Due to the denseness of X_n in $L^2(\Gamma)$ and of Z_n in $C^2(\Omega)$ there exists $\phi_n^* \in X_n$, $r_n^* \in Z_n$ with

$$\|\phi^* - \phi_n^*\|_{L^2(\Gamma)} \to 0, \quad n \to \infty, \tag{3.2}$$

$$\|r^* - r_n^*\|_{C^{1,\beta}(\Omega)} \to 0, \quad n \to \infty. \tag{3.3}$$

It remains to show that for all n large enough, r_n^* can be chosen so that the corresponding surface $\Lambda_n^* \in U_n$, i.e., the conditions (2.9) are fulfilled for r_n^*. We leave out the technical details of the necessary modifications on r_n^* such that (3.3) still holds.

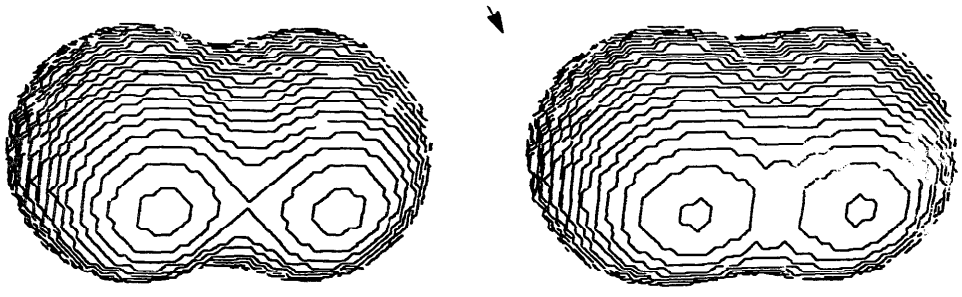

(a) (b)

Fig. 1. The peanut and its reconstruction (turned by 90°); (a) original; (b) reconstruction.

As a consequence of the convergence (3.2) and (3.3) with the aid of the triangle inequality we can deduce that

$$\mu_n \leq \mu(\phi_n^*, \Lambda_n^*) \leq \mu(\phi^*, \Lambda^*) + o(1), \quad n \to \infty,$$

which proves $\mu_n \to \mu$, $n \to \infty$.

From the compactness of U and the boundedness of (ϕ_n), as in the proof of the convergence result of Theorem 2.1, one can deduce the existence of convergent subsequences $\Lambda_{n(j)} \to \Lambda \in U$ and $\phi_{n(j)} \to \phi \in L^2(\Gamma)$, $j \to \infty$. Each accumulation point (ϕ, Λ) is a solution of (2.10) or (2.14), respectively, since

$$\mu(\phi^*, \Lambda^*) \leq \mu(\phi, \Lambda) \leq \mu(\phi_{n(j)}, \Lambda_{n(j)}) \leq \mu(\phi^*, \Lambda^*) + o(1), \quad j \to \infty. \qquad \square$$

The finite-dimensional minimization problem is a nonlinear least-squares problem with $2(n+1)^2$ unknowns. For its numerical solution we used a Levenberg–Marquardt algorithm as one of the most efficient nonlinear least-squares routines. It does not allow the imposition of constraints, but we found in practice that the constraints are unnecessary due to the increase in the cost functional as Λ approaches Γ or tends to infinity or approaches Γ_{meas}.

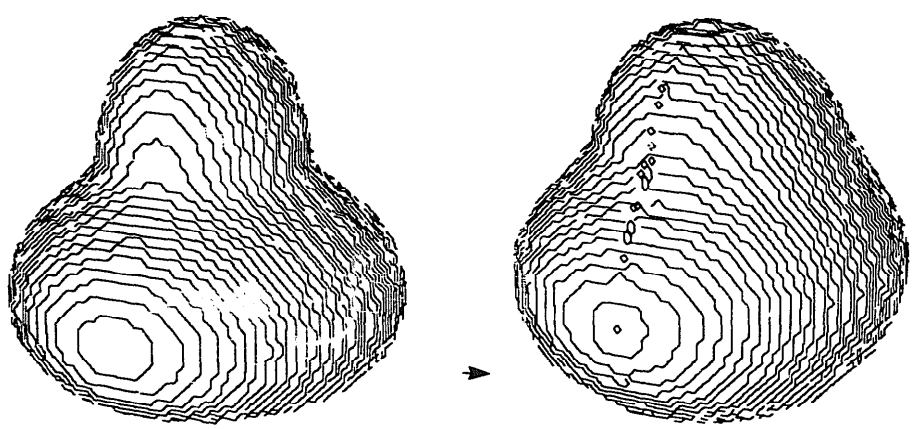

(a) (b)

Fig. 2. The acorn and its reconstruction; (a) original; (b) reconstruction.

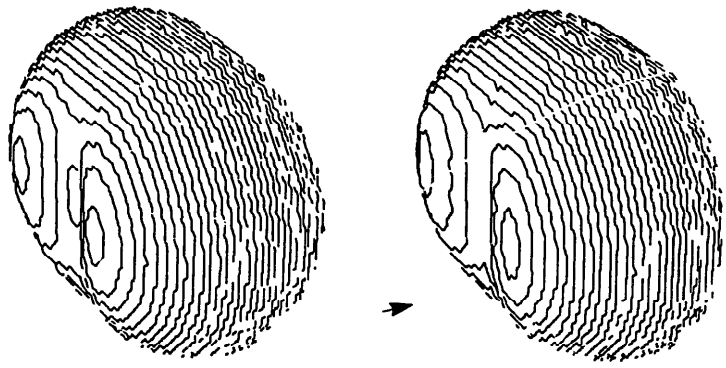

Fig. 3. The pinched ball and its reconstruction; (a) original; (b) reconstruction.

Figures 1–3 show three examples of our numerical experiments. For these the measurement surface Γ_{meas} is a sphere of radius R centered at the origin. In the figures this radius is chosen to be $R = 3$. The regularization parameter α and the coupling parameter γ were selected by trial and error. The actual numerical values were $\alpha = 10^{-8}$ and $\gamma = 10^{-6}$ for the reconstruction from far-field data and, due to the factor $1/R^2$ in the first term of the cost functional, $\alpha = 10^{-8}/R^2$ and $\gamma = 10^{-6}/R^2$ in the case of near-field data. For the internal surface Γ we chose ellipsoids with center at the origin and axes coinciding with the axes of the Cartesian coordinates. As the starting surface Λ for the Levenberg–Marquardt algorithm we used an ellipsoid parallel and with distance 0.2 from Γ, and as the starting density we chose $\phi = 0$. The average number of Levenberg–Marquardt steps was ten. In all examples we worked with only one incident plane wave with the wave number $k = 1$. In the figures the arrow marks the direction of the incident wave. The parameter for the numerical quadrature is $m = 12$ and the dimension of the approximating subspace is $n = 6$.

Figure 1 shows the reconstruction of a peanut given through its radial distance in terms of the polar angle θ by

$$r(\theta) = \tfrac{3}{2}\left(\cos^2\theta + \tfrac{1}{4}\sin^2\theta\right)^{1/2}.$$

The internal ellipsoid has major axis 0.6, 0.6 and 1.2.

Figure 2 shows the reconstruction of an acorn given by

$$r(\theta) = \tfrac{3}{5}\left(\tfrac{17}{4} + 2\cos 3\theta\right)^{1/2}.$$

Here the internal ellipsoid is a sphere with radius 0.6.

Figure 3 shows the reconstruction of a pinched ball given by

$$r(\theta, \phi) = \left(1.2^2 + 0.5\cos 2\phi\,(\cos 2\theta - 1)\right)^{1/2}.$$

Its special feature is that it is rotationally nonsymmetric with respect to the x_3-axis in contrast to all other objects reconstructed before by Colton and Monk [5] and us. Furthermore it is nonconvex. So clearly it is more difficult to reconstruct. Here the internal ellipsoid has major axis 0.5, 1.3 and 1.

Besides these figures we wish to illustrate our results by a few numerical values. In Table 1 we have compared the reconstruction from near-field data with those from far-field data. The

Table 1
Numerical results for the peanut, the acorn and the pinched ball

Radius of Γ_{meas}	Peanut		Acorn		Pinched ball	
	Final value for μ	Error %	Final value for μ	Error %	Final value for μ	Error %
∞	$1.96 \cdot 10^{-6}$	1.93	$8.12 \cdot 10^{-5}$	8.23	$1.10 \cdot 10^{-4}$	6.24
10	$1.96 \cdot 10^{-8}$	1.83	$8.35 \cdot 10^{-7}$	9.51	$4.03 \cdot 10^{-6}$	6.20
5	$7.96 \cdot 10^{-8}$	1.27	$3.72 \cdot 10^{-6}$	10.55	$1.66 \cdot 10^{-5}$	5.55
4	$1.26 \cdot 10^{-7}$	0.74	$6.48 \cdot 10^{-6}$	10.17	$2.63 \cdot 10^{-5}$	5.09
3	$2.31 \cdot 10^{-7}$	0.85	$1.67 \cdot 10^{-5}$	8.86	$4.92 \cdot 10^{-5}$	3.54
2	$7.75 \cdot 10^{-7}$	1.15	$2.57 \cdot 10^{-4}$	7.32	$1.40 \cdot 10^{-4}$	2.10

Table 2
Numerical results for the acorn with perturbed data

Noise ϵ%	Final value for μ	Error %
0	$8.1158 \cdot 10^{-5}$	8.23
2	$8.1219 \cdot 10^{-5}$	8.12
4	$8.1272 \cdot 10^{-5}$	11.06
6	$8.1302 \cdot 10^{-5}$	11.32
8	$8.1342 \cdot 10^{-5}$	11.72
10	$8.1387 \cdot 10^{-5}$	10.75

latter are incorporated in the table through $R = \infty$. Our error is defined as $\| r_{approx} - r^* \| / \| r^* \|$ where the L^2-norm is taken, where r_{approx} represents the boundary for the numerical reconstruction and where r^* denotes the best approximation to the exact boundary r with respect to Z_n. Our results indicate that despite the decrease in the degree of the ill-posedness, the quality of the reconstruction is not much affected by going from far-field to near-field data.

Table 2 shows the influence of perturbed data on the reconstruction of the acorn. We have added a random error to the far-field pattern by adding uniformly distributed random numbers in the range $[-\epsilon, \epsilon]$ to each far-field value. The results indicate that we have developed a stable algorithm for the inverse obstacle scattering problem.

We wish to mention that the accuracy is not much improved by using two incident plane waves with different directions instead of only one wave. We have not implemented (2.11) with more than two waves since the computational costs are too high. Computations with one wave as a combination of several incident fields have been carried out, but up to now the reconstructions have not improved as remarkably as expected.

The computations were carried out on a DECstation 3100. The typical CPU-time for one reconstruction varied between 5 and 10 minutes.

References

[1] T.S. Angell, D. Colton and A. Kirsch, The three dimensional inverse scattering problem for acoustic waves, *J. Differential Equations* **46** (1982) 46–58.

[2] D. Colton and R. Kress, *Integral Equation Methods in Scattering Theory* (Wiley, New York, 1983).
[3] D. Colton and P. Monk, A novel method for solving the inverse scattering problem for time-harmonic acoustic waves in the resonance region, *SIAM J. Appl. Math.* **45** (1985) 1039–1053.
[4] D. Colton and P. Monk, A novel method for solving the inverse scattering problem for time-harmonic acoustic waves in the resonance region II, *SIAM J. Appl. Math.* **46** (1986) 506–523.
[5] D. Colton and P. Monk, The numerical solution of the three dimensional inverse scattering problem for time-harmonic acoustic waves, *SIAM J. Sci. Statist. Comput.* **8** (1987) 278–291.
[6] D. Colton and B.D. Sleeman, Uniqueness theorems for the inverse problem of acoustic scattering, *IMA J. Appl. Math.* **31** (1983) 253–259.
[7] D.S. Jones, Note on a uniqueness theorem of Schiffer, *Appl. Anal.* **19** (1985) 181–188.
[8] A. Kirsch and R. Kress, An optimization method in inverse acoustic scattering, in: C.A. Brebbia et al., Eds., *Boundary Elements IX, Vol. 3. Fluid Flow and Potential Applications* (Springer, Heidelberg, 1987) 3–18.
[9] A. Kirsch, R. Kress, P. Monk and A. Zinn, Two methods for solving the inverse acoustic scattering problem, *Inverse Problems* **4** (1988) 749–770.
[10] R. Kress, *Linear Integral Equations* (Springer, New York, 1989).
[11] G. Kristensson and C.R. Vogel, Inverse problems for acoustic waves using the penalised likelihood method, *Inverse Problems* **2** (1986) 461–479.
[12] L. Misici and F. Zirilli, An inverse problem for the three dimensional Helmholtz equation with Neumann or mixed boundary conditions, in: G. Cohen et al., Eds., *Mathematical and Numerical Aspects of Wave Propagation Phenomena* (SIAM, Philadelphia, PA, 1991) 497–508.
[13] R.D. Murch, D.G.H. Tan and D.J.N. Wall, Newton–Kantorovich method applied to two-dimensional inverse scattering for an exterior Helmholtz problem, *Inverse Problems* **4** (1988) 1117–1128.
[14] K. Onishi, Numerical methods for inverse scattering problems in two-dimensional scalar field, to appear.
[15] O. Pironneau, *Optimal Shape Design for Elliptic Systems* (Springer, New York, 1984).
[16] A. Roger, Newton Kantorovitch algorithm applied to an electromagnetic inverse problem, *IEEE Trans. Antennas and Propagation* **AP-29** (1981) 232–238.
[17] S.L. Wang and Y.M. Chen, An efficient numerical method for exterior and interior inverse problems of Helmholtz equation, to appear.
[18] L. Wienert, Die numerische Approximation von Randintegraloperatoren für die Helmholtzgleichung im $\mathbb{R}^3$, Dissertation, Univ. Göttingen, 1990.
[19] A. Zinn, On an optimisation method for the full- and limited-aperture problem in inverse acoustic scattering for a sound-soft obstacle, *Inverse Problems* **5** (1989) 239–253.
[20] A. Zinn, Ein Rekonstruktionsverfahren für ein inverses Streuproblem bei der zeitharmonischen Wellengleichung, Dissertation, Univ. Göttingen, 1990.